

1 **Title & running title:** Distance sampling with camera traps

2 **Word count** (excluding this page): 6998

3 **Authors:** Eric J. Howe^{1*}, Stephen T. Buckland¹, Marie-Lyne Després-Einspinner², Hjalmar S.

4 Kühl^{2,3}

5

6 ¹ Centre for Research into Ecological and Environmental Modelling, University of St Andrews,

7 The Observatory, Buchanan Gardens, St Andrews, Fife KY16 9LZ, UK

8 ² Max Planck Institute for Evolutionary Anthropology, Deutscher Platz 6, 04103, Leipzig,

9 Germany

10 ³ German Centre for Integrative Biodiversity Research (iDiv) Halle-Jena-Leipzig, Deutscher

11 Platz 5e, 04103 Leipzig, Germany

12 * Correspondence author. E-mail: ejh20@st-andrews.ac.uk

13

14 **Summary**

15 **1.** Reliable estimates of animal density and abundance are essential for effective wildlife
16 conservation and management. Camera trapping has proven efficient for sampling multiple
17 species, but statistical estimators of density from camera trapping data for species that cannot be
18 individually identified are still in development.

19 **2.** We extend point-transect methods for estimating animal density to accommodate data from
20 camera traps, allowing researchers to exploit existing distance sampling theory and software for
21 designing studies and analyzing data. We tested it by simulation, and used it to estimate
22 densities of Maxwell's duikers (*Philantomba maxwellii*) in Taï National Park, Côte d'Ivoire.

23 **3.** Densities estimated from simulated data were unbiased when we assumed animals were not
24 available for detection during long periods of rest. Estimated duiker densities were higher than
25 recent estimates from line transect surveys, which are believed to underestimate densities of
26 forest ungulates.

27 **4.** We expect these methods to provide an effective means to estimate animal density from
28 camera trapping data and to be applicable in a variety of settings.

29

30 **Keywords:** animal abundance, camera trapping, density, distance sampling, Maxwell's duiker

31

32 **Introduction**

33 Remote motion-sensitive photography, or camera trapping, is increasingly used in
34 wildlife research, and allows multiple research objectives to be addressed (Sollmann et al. 2013a,
35 Burton et al. 2015, Rovero and Zimmermann 2016). Estimation of population density (D) is a
36 key objective of many ecological studies and assessments of conservation status employing

37 camera traps (Burton et al. 2015, Rovero and Zimmermann 2016). If individuals are
38 recognizable, density can be estimated using spatially explicit capture–recapture (SECR) models
39 (Efford et al. 2009), but methods for estimating D from camera trapping data in the absence of
40 individual identification are still in development (Sollmann et al. 2013a, Burton et al. 2015,
41 Dénes et al. 2015, Rovero and Zimmermann 2016). Detection rates at camera traps have been
42 used to index abundance, but indices can rarely be converted to estimates of absolute density,
43 and spatiotemporal variation in detection rates does not provide reliable evidence of differences
44 or trends in abundance (Sollmann et al. 2013b, Burton et al. 2015). The random encounter
45 model (REM) estimates absolute density as a function of the detection rate, the dimensions of a
46 sector within which detection is certain, and the speed of animal movement; methods for
47 quantifying the latter two parameters from camera trapping data have been described (Rowcliffe
48 et al. 2008, 2011, 2016). The REM has been recognized as a potentially useful model, but its
49 accuracy and reliability remains to be demonstrated (Rovero and Marshal 2009, Sollmann et al.
50 2013a, Zero et al. 2013, Cusack et al. 2015a, Balestrieri et al. 2016, Caravaggi et al. 2016).
51 SECR estimators for unmarked populations estimate the number and location of animals' activity
52 centers from the spatial correlation of counts at different sampling locations; sampling must be
53 sufficiently intensive to detect the same animals at multiple locations, and estimates lack
54 precision (Chandler and Royle 2013).

55 Here we describe how densities of unmarked animal populations can be estimated by
56 distance sampling (DS) with camera traps, allowing researchers to take advantage of a well-
57 described theoretical framework complete with software and advice for designing studies and
58 analyzing data (Buckland et al. 2001, 2004, 2015, Thomas et al. 2010, Miller 2015,
59 distancesampling.org). Below, we formulate a point transect distance sampling model specific to

60 camera traps and describe its assumptions and the estimation of variances. We test for bias in
 61 estimated density (\hat{D}) and its variance by simulation, and apply the method to estimate the
 62 density of Maxwell's duikers (*Philantomba maxwellii*) in Taï National Park, Côte d'Ivoire.

63

64 **Methods**

65 *Formulation of the Model*

66 A camera trap (CT) is deployed at a point k that is independent of animal density for a
 67 period of time T_k and set to record images for as long as an animal is present to trigger it. We
 68 predetermine a finite set of snapshot moments within T_k , t units of time apart, at which an image
 69 of an animal could be obtained. Temporal effort at the point is then T_k / t . When images of
 70 animals are obtained, we estimate the horizontal radial distance r_i between the midpoint of each
 71 animal and the camera, at each snapshot moment, for as long as it remains in view. If the camera
 72 covers an angle θ radians, then $\frac{\theta}{2\pi}$ describes the fraction of a circle covered by the camera, so we
 73 define overall sampling effort at point k as $\frac{\theta T_k}{2\pi t}$. We regard the data as a series of snapshots, and
 74 density estimation follows by standard point transect methods (Buckland et al. 2001). We
 75 estimate D as

$$76 \quad \hat{D} = \frac{\sum_{k=1}^K n_k}{\pi w^2 \sum_{k=1}^K e_k \hat{P}_k} \quad (1)$$

77 where $e_k = \frac{\theta T_k}{2\pi t}$ is the effort expended at point k , K is the set of points, θ is the horizontal angle
 78 of view (AOV) of the camera, w is the truncation distance beyond which any recorded distances
 79 are discarded, n_k is the number of observations of animals in the population of interest at point k ,
 80 and \hat{P}_k is the estimated probability of obtaining an image of an animal that is within θ and w in
 81 front of the camera at a snapshot moment.

82 . Substituting e_k in (1), we have

$$83 \quad \hat{D} = \frac{2t \sum_{k=1}^K n_k}{\theta w^2 \sum_{k=1}^K T_k \hat{P}_k} \quad (2)$$

84 We use the distances r_i to model the detection function and hence to estimate P_k .

85

86 *Assumptions and Practical Considerations*

87 The usual DS assumptions apply (see Chapter 2 of Buckland et al. 2001). We record
 88 distances at instantaneous snapshot moments to ensure that animal movement does not bias the
 89 distribution of detection distances. Below, we describe an approach for accurately assigning
 90 animals to distance intervals; Rowcliffe et al. (2011) and Caravaggi et al. (2016) describe
 91 methods for measuring continuous distances between CTs and detected animals.

92 Random designs or systematic designs with random origin are consistent with the
 93 assumption that points are placed independently of animal locations. Selecting camera
 94 orientations as part of the design is also advisable. Orientations could be selected randomly, or
 95 the same orientation could be used for all cameras. Deviating slightly from the location and
 96 orientation selected by design (e.g., to attach the camera to a nearby tree or to avoid an obscured
 97 field of view) would not bias estimates provided field staff do not intentionally target habitat
 98 features known to be either preferred or avoided by the animals.

99 Empirical, design-based estimators of the encounter rate variance are robust to violation
 100 of the assumption that detections are independent events (Fewster et al. 2009, Buckland et al.
 101 2015). However, in CT surveys we expect violations to be severe because we include multiple
 102 detections of the same animal during a single pass through the detection zone. We can avoid this
 103 assumption by estimating variances using a nonparametric bootstrap, resampling points with
 104 replacement (Buckland 1984, Buckland et al. 2001). Another consequence of lack of

105 independence is that the usual goodness-of-fit tests and model selection criteria are invalid
106 (Buckland et al. 2001). Methods for selecting among DS models when observations are not
107 independent are in development.

108 The assumption that detection is certain at zero distance could be violated by (1) animals
109 passing beneath the field of view (FOV) of the camera, (2) failure to identify the species because
110 only part of the animal is visible, and possibly (3) the delay between the time the sensor is
111 activated and the time the first image is recorded (the “trigger speed”), if animals directly in front
112 of the camera at a snapshot moment do not yield images. Such violations may be detectable
113 during exploratory analysis in the form of fewer than expected detections near the point, and bias
114 can be avoided via left-truncation (Buckland et al. 2001, Marques et al. 2007, e.g. Obbard et al.
115 2015). To minimize violations and ensure that detection probability is certain or high at some
116 distance near the point, cameras should be set at a height appropriate to the species of main
117 interest (Rovero and Zimmermann 2016). Lower heights would reduce the chance of small
118 animals passing beneath the camera at short distances, but would also reduce the range of
119 distances over which animals could be detected and therefore sample size and flexibility when
120 modelling the detection function. Pairs of CTs triggered by passive infrared (PIR) sensors and
121 mounted at the same location, height, and orientation, or one PIR CT deployed in combination
122 with other sampling devices (track plots, CTs triggered by pressure plates or active IR sensors)
123 could facilitate field tests of whether or not detection probability is close to 1 at short distances in
124 front of PIR CTs. Paired cameras mounted some distance apart targeting the same location
125 would not provide an effective test, but would provide the data needed to apply mark–recapture
126 distance sampling methods, which avoid this assumption (Buckland et al. 2004, Laake et al.
127 2011).

128 In traditional point transect surveys, human observers measure distances to each detected
129 animal only once during each visit to a point, and effort at each point is the number of times it
130 was visited. CTs remain at the point, but the snapshot approach discretizes the number of times
131 we could potentially detect each animal (as T_k/t as described above). However, CTs detect only
132 moving animals within the range of the sensor and the FOV of the camera, and can be
133 programmed to record multiple still images, or video footage, each time the sensor is triggered
134 (Rovero and Zimmermann 2016). These characteristics of CTs as observers must be taken into
135 consideration. Observed distances upon first detection are expected to be positively biased
136 because animals entering the detection zone through the arc of the sector would contribute a
137 disproportionate number of observations at far distances. Bias would be slight if the time
138 between snapshot moments (t) was small enough to ensure that the animals did not move far
139 relative to the range of the sensor between snapshots, as then the observations would be
140 representative of animals' continuous paths past the CTs. However, we prefer to avoid the
141 potential for bias by assuming that the snapshot moments are selected independently of animal
142 locations, and predetermining them as specific times of day to ensure that the assumption is met.
143 Practical considerations constrain t . If t is large, animals that trigger the sensor might leave the
144 detection zone before a snapshot moment arises, which would not cause bias but wastes data. As
145 t is reduced, there would be fewer missed detections and larger samples as we record distance to
146 each animal multiple times during a single pass in front of the CT. Eventually, improvements in
147 the precision of \hat{D} with larger samples would become negligible because variation in the
148 encounter rate among points would contribute most of the variation in estimated density.
149 Reducing t further would then needlessly increase the time required to process and analyze the
150 data. We suggest that values from 0.25 to 3 seconds are likely to be useful, with values at the

151 lower end of the range being more appropriate for faster-moving or rarer animals, and CTs with
152 faster trigger speeds.

153 Programming cameras to record time-stamped video would make it straightforward to
154 record distances at the predetermined snapshot moments. If still images are preferred, cameras
155 should be programmed to record an image at the next several snapshot moments when triggered,
156 or, if this is not feasible, to record a rapid series or “burst” of still images to ensure that images
157 are recorded at times that align with snapshot moments. There should always be the potential for
158 the camera to be triggered again immediately or after a minimal delay. Note that depending how
159 cameras are programmed, the sample of distances observed in CT data may or may not comprise
160 a realization from the detection function described by the probability that an animal at distance r
161 triggers the sensor. If cameras record a single image at the subsequent snapshot moment, or a
162 rapid series of images for $< t$ seconds, when the sensor is triggered, then each detection of an
163 animal that triggers the sensor several times during a pass in front of a CT is a function of the
164 sensitivity of the sensor. If cameras are set to record video, or a series of still images for $> 2t$
165 seconds, then all but the first detection is certain for as long as the animal remains in the FOV
166 and the camera continues to record images. Furthermore, regardless of how the camera is
167 programmed, any other animals in the FOV while the camera is recording images would
168 contribute observations that do not depend on the sensitivity of the sensor. These differences do
169 not invalidate the method provided we define the detection function as representing the
170 proportion of locations at different distances which are recorded, regardless of whether an animal
171 triggered the sensor at that distance.

172 Obviously, we can only estimate the density of populations that are available for
173 detection by CTs. Similarly, because the sampling duration at each location (T_k) is part of the

174 model definition, we expect densities of animals that spend part of their time outside the vertical
175 range of camera traps to be underestimated, and for the bias to be proportional to time animals
176 are not available for detection. For example, with T_k set to the study duration, we expect \hat{D} of a
177 species that spends all its time in the canopy to be zero, and of a species that spends half its time
178 underground and the rest at ground level to be half of the true density. Negative bias would also
179 result if animals went undetected only because movement was insufficient to trigger the sensor.
180 To avoid this bias, either T_k should be defined as the amount of time that the entire population
181 was available for detection while cameras were operating, or, equivalently, the proportion of
182 time when animals were available for detection should be included as a parameter in the model.
183 Animals are unavailable for detection when outside the vertical range of CTs, and may not be
184 available when within this range depending on their level of activity. We explore this issue
185 further in subsequent sections.

186

187 *Simulations*

188 We tested the method using simulations employing simple and complex models of animal
189 movement and different sampling scenarios (see supplemental material). With the simple model,
190 animals moved continuously at a constant speed and tended to maintain their heading. The
191 complex model included variable speeds and tortuosities, and all animals rested for the same 12
192 hours of each day. We recorded the distance between cameras and animals within detection
193 zones every two seconds, 24 hours per day. Where the complex model was used, we also
194 collected data only when animals were moving, and reduced T_k by half accordingly when
195 estimating density.

196

197 *Example: Maxwell's duikers in Tai National Park*

198 We used point transect DS methods to estimate the density of Maxwell's duikers within
199 the territory of the "east group" habituated chimpanzee community in Tai National Park, Côte
200 d'Ivoire (Després-Einspenner et al. accepted; Fig 1a). Maxwell's duikers were sampled from 28-
201 June through 21-Sept, 2014 at 23 camera traps (Bushnell Trophy CamTM; Model 119576C)
202 mounted at a height of 0.7 – 1.0 m and set to high sensitivity. Cameras were deployed with a
203 fixed orientation of 0° at the intersections of a grid with 1 km spacing and a random origin
204 superimposed over the study area (Fig. 1b). Realized sampling locations and orientations
205 deviated from the design by as much as 30 m, and 40°, respectively, in order to mount cameras
206 on trees and to ensure there was some chance of detecting animals. During installation of each
207 camera, we measured horizontal radial distances from the camera, and recorded videos of
208 researchers holding distance markers, at 1 m intervals out to 15 m, in the center and along both
209 sides of the FOV. We estimated distances to filmed duikers by comparing their locations to
210 those of researchers in the reference videos. We set $t = 2$ seconds, and recorded the distance
211 interval within which the midpoint of each animal fell at 0, 2, 4, ... , 58 seconds after the minute.
212 Larger distances were more difficult to measure precisely, so we assigned animals to 1-m
213 intervals out to 8 m, but binned observations between 8 and 10 m, 10 and 12 m, 12 and 15 m,
214 and beyond 15 m.

215 We excluded data from one camera because the FOV was largely obscured by vegetation,
216 and another which was placed on a slope and failed to detect any animals, but we included data
217 from a third camera that functioned normally but did not detect any duikers. Maxwell's duikers
218 sleep or rest for most of each night and for shorter periods during the day (Newing 1994, 2001).
219 We assumed they would not be available for detection overnight and excluded the hours of

220 darkness (19:00 – 6:00) from T_k *a-priori*. We accounted for limited availability during the
 221 daytime three different ways. First we naively assumed that all duikers were active by 6:30:00
 222 and remained so through 17:59:59, included distances observed during this interval in a
 223 “daytime” data set, and defined temporal effort at each location (T_k / t) as the number of 2-
 224 second time steps during that time interval (20699), multiplied by the number of sampling days.
 225 Second, we assumed that all animals were available only during apparent times of peak activity
 226 (6:30:00 – 8:59:59 and 16:00:00 – 17:59:59) and recalculated temporal effort and censored
 227 distance observations accordingly (T_k / t per day = 8098). Third, we defined T_k and included
 228 observations as above for the daytime data set, and included an independent estimate of the
 229 proportion of time captive Maxwell’s duikers were active during the same time interval (0.64;
 230 Newing et al. 2001) in the denominator of Eq. 2. We included only data from complete days
 231 when cameras were operating and not visited by researchers.

232 We fit point transect models in program Distance (version 7.0; Thomas et al. 2010),
 233 defining survey effort at each location as $\frac{\theta T_k}{2\pi t}$. The cameras had an AOV of 42°, and a wider
 234 effective angle of the sensor (Trailcampro.com 2015), so we set $\theta = 42^\circ$ or 0.733 radians. We
 235 considered models of the detection function with the half-normal key function with 0, 1 or 2
 236 Hermite polynomial adjustment terms, the hazard rate key function with 0, 1, or 2 cosine
 237 adjustments, and the uniform key function with 1 or 2 cosine adjustments. Adjustment terms
 238 were constrained, where necessary, to ensure the detection function was monotonically
 239 decreasing. We selected among candidate models of the detection function by comparing AIC
 240 values, acknowledging the potential for overfitting because many observations were not
 241 independent. We present measures of uncertainty derived from design-based variances (“P2” of

242 Fewster et al. 2009, Web Appendix B), and from 999 bootstrap resamples, with replacement,
243 across camera locations.

244

245 **Results**

246 *Simulations*

247 Where we used the simple model of animal movement, and where we used the complex
248 model of animal movement and collected data only when animals were active, \hat{D} was unbiased
249 (Table S1). Results were biased and erratic when we recorded distances to resting animals (see
250 supplemental material for details). Design-based variances were smaller than the sampling
251 variance of \hat{D} across iterations, and associated confidence interval coverage was <90% (Table
252 S1). Where we estimated variance by bootstrapping, the coefficient of variation was 0.119,
253 similar to the sampling variance of \hat{D} , and CI coverage was 93.6% across 1000 iterations.
254 Doubling spatial sampling effort improved precision, slightly more so where we doubled the
255 number of locations as opposed to θ (Table S1).

256

257 *Example: Maxwell's duikers in Tai National Park*

258 We obtained 11324 observations of the distance between Maxwell's duikers and cameras
259 in 806 different videos. Duikers were rarely filmed during hours of darkness. The frequency of
260 detection increased steadily after 6:00 to a maximum between 6:30 and 7:00 and remained
261 relatively high until 9:30, after which it decreased slightly and remained relatively low until
262 16:30, then increased again and remained high until 18:00, then declined gradually until 19:00
263 (Fig. 2). Duikers were always active when detected; CTs did not record any duikers that were

264 asleep or stationary for an entire minute. We recorded 11180 distances from 6:30:00 through
265 17:59:59, and 6274 during times of peak activity.

266 Exploratory analyses revealed no evidence of data collection errors, and a paucity of
267 observations between 1 and 2 m but not between 2 and 3 m, so we left-truncated at 2 m. Fitted
268 detection functions and probability density functions were heavy-tailed when distances > 15 m
269 were included, so we right-truncated at 15 m. Truncating removed 8% of observations from the
270 daytime data set, leaving $n = 10284$, and 6.5% of observations from the peak activity data set,
271 leaving $n = 5865$. Mean encounter rates (mean numbers of duikers observed per 2-second time
272 interval) across all points were 3.27×10^{-4} during the daytime and 4.76×10^{-4} during times of
273 peak activity. Encounter rates were highly variable among locations but did not exhibit an
274 obvious spatial pattern across the study area, and there was no evidence of spatial autocorrelation
275 (Moran's $I P = 0.47$; Fig. 3).

276 When we fit the hazard rate model with two adjustment terms to the daytime data set, the
277 detection function was not monotonically decreasing, so this model was not considered for
278 estimation. All models were fitted successfully to the peak activity data set. The hazard rate
279 model with no adjustments minimized AIC and was used to estimate density in both cases.
280 Probability density functions of observed distances and relationships between detection
281 probability and distance were similar (Fig. 4). Detection probability was ~ 1.0 within 5 m and
282 0.05 at 15 m; effective detection radii were 9.1 and 9.4 m from the daytime and peak activity
283 data sets, respectively.

284 We expected to underestimate density where we assumed duikers were active all day; \hat{D}
285 was 37% higher when we included only data from times of peak activity (Table 1). Including an
286 independent estimate of the proportion of time active during the daytime as a parameter in the

287 model fit to the daytime data set yielded a still higher estimate (“Active daytime” in Table 1).
288 Measures of uncertainty in the proportion of time active were not available (Newing et al. 2001)
289 so did not contribute to the variance of \hat{D} . Bootstrap variances were larger than design-based
290 analytic variances (Table 1). The vast majority (99.8%) of the design-based variance of \hat{D} was
291 attributable to the variation in encounter rate between locations, and only 0.2% to detection
292 probability.

293

294 **Discussion**

295 Simulations demonstrated the potential for the method to yield unbiased density
296 estimates, but also that animals’ activity patterns must be accounted for. Where simulated
297 animals rested for half of each day and we set T_k equal to the survey duration, the most common
298 scenario was that animals did not rest in front of CTs and negative bias in \hat{D} was proportional to
299 the time spent resting. When we recorded distance at each snapshot moment while animals
300 rested in front of CTs, the encounter rate and therefore \hat{D} was higher on average, but the shape of
301 the detection function was strongly affected, leading to erratic estimates and cases where models
302 could not be fitted to the data. In practice, it is unlikely that we would detect animals while they
303 sleep or rest because movement will be insufficient to trigger the sensor. Therefore, estimates of
304 the proportion of time animals are active within the vertical range of CTs will be required to
305 avoid negatively biased \hat{D} . Ideally, this proportion would be estimated from data collected
306 concurrently with the distance data to ensure it is representative. Fortunately, the temporal
307 distribution of camera trap detections is informative regarding animal activity patterns (Lynam et
308 al. 2013, Cruz et al. 2014, Rowcliffe et al. 2014). If it is reasonable to assume that the entire
309 population is available for detection for any part of each day, additional data would not be

310 required to estimate \hat{D} accurately, because we could either (1) analyze only the data collected at
311 that time, censoring effort and distance data from other times, or (2) estimate the overall
312 proportion of time active directly from the CT data (e.g. Rowcliffe et al. 2014). Newing's (1994)
313 data from Tai indicated that there was no time at which all wild duikers could be assumed to be
314 active. If this was true during our survey, we may have underestimated density where we did not
315 correct for limited availability within the time included in T_k , because even at times of peak
316 activity some animals may have been resting and unavailable for detection. Activity data from
317 wild duikers were presented only as figures and could not be converted into estimates of the
318 overall proportion of time active (Newing 1994). We therefore relied on the assumption that
319 activity data from captive duikers (Newing 1994, Newing et al. 2001) were representative of
320 activity patterns during our survey. If this assumption held, then the density estimate calculated
321 using their estimate of the proportion of time active during the day should not be biased as a
322 result of limited availability. We suggest that the need to account for availability should not pose
323 a serious obstacle to reliable estimation of the density of many species, but for others, notably
324 ectotherms, and semi-arboreal and fossorial species, it will require careful consideration, and
325 possibly additional data. We further suggest that combining Rowcliffe et al.'s (2014) or similar
326 methods for estimating the proportion of time active from detection times at CTs with the point
327 transect method described here could yield accurate density estimates for many species from CT
328 data alone.

329 Avoidance of, or attraction to, CTs would bias encounter rates and therefore density
330 estimates. Some species exhibit complex responses to CTs or are particularly wary of humans
331 (Séquin et al. 2003). If behavioural responses are expected or apparent in images of detected
332 animals, CTs could be deployed prior to the start of the actual survey to allow animals to become

333 accustomed to them and for signs of human presence to dissipate. Similarly, effort and distance
334 data from times when animals may have been displaced from the trap sites by humans visiting
335 them to download data, replace batteries, etc., should be censored.

336 The probability of detection at PIR CTs is lower at greater angles from the center of the
337 FOV, due to a combination of the trigger speed, the effective horizontal angle of the sensor
338 relative to the AOV of the camera (which varies among CT models) and possibly reduced
339 sensitivity of the sensor at the periphery of its horizontal range (Rowcliffe et al. 2011, Rovero et
340 al. 2013, Rovero and Zimmermann 2016). This introduces heterogeneity in the detection
341 function. Fortunately, provided that detection is certain at zero distance, the pooling robustness
342 property ensures that estimation is unbiased in the presence of heterogeneity in detectability
343 among individuals (Buckland et al. 2004), and this also applies to heterogeneity caused by
344 differences in angle at different snapshot moments. However, if detection probability at high θ
345 is much lower than in the centre, fitted models of the detection function might show a rapid drop
346 in detection probability near the point, whereas detection functions with a gradual decrease near
347 the point are preferred for stable density estimation (Buckland et al. 2001). The expected
348 distribution of angles within a sector within which the sensor is fully effective is uniform. We
349 recommend that researchers measure angles as well as distances to detected animals (e.g.
350 Carravaggi et al. 2016), and test for departures from the uniformity assumption at increasing
351 angles as part of their exploratory analysis. If departures are apparent, the data could be
352 truncated to exclude observations beyond an angle within which the distribution is approximately
353 uniform, in which case θ should be set to two times the truncation angle rather than the AOV of
354 the camera in the definition of effort. An alternative approach that would allow us to retain all of
355 the data would be to develop a two dimensional detection function where detection probability

356 depends on both radial distance and angle from center, using methods similar to those developed
357 by Marques et al. (2010). We expect heterogeneity with angle to be more severe with CT
358 models with narrow horizontal ranges of the sensor relative to the AOV of the camera, or slow
359 trigger speeds, and where faster-moving animals are sampled. CTs with fast trigger speeds, short
360 recovery times, and curved array Fresnel lenses (which provide a wide effective angle of
361 detection such that the camera begins recording images as or even before the animal enters the
362 FOV; Rovero and Zimmermann 2016) could reduce or eliminate differences in detection
363 probability at different angles in future studies.

364 The encounter rate variance accounted for the vast majority of the design-based variance
365 in duiker density, and variances around \hat{D} were larger than for simulated data despite similar
366 sample sizes. Real populations exhibit clumped or patchy distributions and non-random
367 movement, leading to variable encounter rates among sampling locations and hence greater
368 uncertainty in \hat{D} (Buckland et al 2001, Fewster et al. 2009); the small area sampled at each
369 location exacerbates this problem. Increasing the area sampled will therefore enhance precision,
370 more so than would increasing temporal effort at a point. Theory predicts that increasing the
371 number of points will yield the largest improvements to precision (Buckland 1984, Fewster et al.
372 2009). That the improvement in precision in simulations was only slightly greater where we
373 doubled the number of sampling locations than where we doubled θ is not representative of real
374 studies because the expected spatial distribution of animal locations was uniform, and movement
375 was random. Coefficients of variation around \hat{D} for duikers were >35% despite large samples of
376 distance observations, so we recommend that future studies employ more points to improve
377 precision.

378 The density of Maxwell's duikers at Tai was recently estimated as 1.6 / km² from line
379 transect DS surveys (N'Goran 2006). However, line transect sampling by human observers is
380 believed to severely underestimate densities of forest-dwelling animals in general, and forest
381 antelopes in particular, due to effects of evasive movement and behaviour in response to
382 observers on both the encounter rate and the distribution of observed distances (Koster and Hart
383 1988, Jathanna et al. 2003, Rovero and Marshall 2004, 2009, N'Goran 2006, Marshall et al.
384 2008, Marini et al. 2009). Estimates of sign density from line transect surveys are frequently
385 converted to estimates of animal density, but this is expected to yield biased estimates in the
386 absence of local and concurrent estimates of sign production and decay rates, which are time-
387 consuming to estimate (Plumptre 2000, Kuehl et al. 2007, Todd et al. 2008). Dung surveys may
388 further require genetic analysis to identify the species (Bowkett et al. 2009). Distance sampling
389 with CTs apparently avoided the underestimation characteristic of line transect surveys of live
390 animals, in less time than would be required to obtain reliable estimates from sign surveys.

391 The recent proliferation of CT studies is providing new information about wildlife in
392 diverse habitats (Burton et al. 2015, Rovero and Zimmermann 2016). Where estimating the
393 density of a rare but individually identifiable species is the primary research objective, it may be
394 preferable to deploy CTs non-randomly in order to obtain sufficient detections of individuals to
395 estimate density by SECR (Wearn et al. 2013, Cusack et al. 2015b, Després-Einspenner et al.
396 accepted). However, multiple research objectives can be addressed, and useful data for multiple
397 species obtained, if CTs are deployed according to a randomized design (MacKenzie and Royle
398 2005, Wearn et al. 2013, Burton et al. 2015, Dénes et al. 2015). The size of unmarked
399 populations can then be estimated from CT data using Poisson and negative binomial GLMs or
400 hierarchical N-mixture models (Dénes et al. 2015), but population density is of greater interest

401 because it is more biologically relevant and comparable across studies. Densities of unmarked
402 animal populations can only be estimated from CT data using SECR models for unmarked
403 populations, the REM, or DS methods; the latter two require randomized designs (Rowcliffe et
404 al. 2008, Buckland et al. 2001). SECR methods for unmarked populations require intensive
405 designs, and even then estimates will often be too imprecise to be useful unless a subset of the
406 population can be reliably identified (Chandler and Royle 2013, Saout et al. 2014). The REM
407 requires an estimate of the average speed of animal movement, assumes that detection is certain
408 within an estimable area in front of the camera, and makes use of only one observation from each
409 detected animal (Rowcliffe et al. 2008). Our point transect approach requires an estimate of the
410 proportion of time animals are available for detection, assumes that detection is certain only at
411 zero distance, and multiple observations from each detected animal inform detection probability
412 estimates. We expect the extension of point transect DS methods to provide an effective and
413 efficient tool for estimating animal density and to enhance the information derived from CT
414 surveys.

415

416 **Acknowledgements**

417 We thank the Robert Bosch Foundation, the Max Planck Society, and the University of St
418 Andrews for funding, the Ministère de l'Enseignement Supérieur et de la Recherche Scientifique
419 and the Ministère de l'Environnement et des Eaux et Forêts in Côte d'Ivoire for permission to
420 conduct field research in Taï National Park, and Dr. Roman Wittig for permitting data collection
421 in the area of the Taï Chimpanzee Project.

422

423 **References**

- 424 Balestrieri A, Ruiz-González A, Vergara M, Capelli E, Tirozzi P, Alfino S, Minuti G, Prigioni C,
425 Saino N. 2016. Pine marten density in lowland riparian woods: a test of the Random Encounter
426 Model based on genetic data. *Mammalian Biology-Zeitschrift für Säugetierkunde*
427 doi:10.1016/j.mambio.2016.05.005
428
- 429 Bowkett AE, Plowman AB, Stevens JR, Davenport TR, van Vuuren BJ. 2009. Genetic testing of
430 dung identification for antelope surveys in the Udzungwa Mountains, Tanzania. *Conservation*
431 *Genetics* 10:251-255
432
- 433 Buckland ST. 1984. Monte Carlo confidence intervals. *Biometrics* 1:811-817
434
- 435 Buckland ST, Anderson DR, Burnham KP, Laake JL, Borchers DL, Thomas L. 2001.
436 Introduction to distance sampling: estimating abundance of biological populations. Oxford
437 University Press, Oxford
438
- 439 Buckland ST, Anderson DR, Burnham KP, Laake JL, Borchers DL, Thomas L. 2004. Advanced
440 distance sampling: estimating abundance of biological populations. Oxford University Press,
441 Oxford
442
- 443 Buckland ST, Rexstad EA, Marques TA, Oedekoven CS. 2015. Distance sampling: methods and
444 applications. Springer, Heidelberg
445

- 446 Burton AC, Neilson E, Moreira D, Ladle A, Steenweg R, Fisher JT, Bayne E, Boutin S. 2015.
447 REVIEW: Wildlife camera trapping: a review and recommendations for linking surveys to
448 ecological processes. *Journal of Applied Ecology* 52:675-85
449
- 450 Caravaggi A, Zaccaroni M, Riga F, Schai-Braun SC, Dick JT, Montgomery WI, Reid N. 2016.
451 An invasive-native mammalian species replacement process captured by camera trap survey
452 random encounter models. *Remote Sensing in Ecology and Conservation* 2:45-58
453
- 454 Chandler RB, Royle JA. 2013. Spatially explicit models for inference about density in unmarked
455 or partially marked populations. *The Annals of Applied Statistics* 7:936-954
456
- 457 Cruz P, Paviolo A, Bó RF, Thompson JJ, Di Bitetti MS. 2014. Daily activity patterns and habitat
458 use of the lowland tapir (*Tapirus terrestris*) in the Atlantic Forest. *Mammalian Biology-
459 Zeitschrift für Säugetierkunde* 79:376-83
460
- 461 Cusack JJ, Dickman AJ, Rowcliffe JM, Carbone C, Macdonald DW, Coulson T. 2015*b*. Random
462 versus game trail-based camera trap placement strategy for monitoring terrestrial mammal
463 communities. *PloS ONE* 10:e0126373
464
- 465 Cusack JJ, Swanson A, Coulson T, Packer C, Carbone C, Dickman AJ, Kosmala M, Lintott C,
466 Rowcliffe JM. 2015*a*. Applying a random encounter model to estimate lion density from camera
467 traps in Serengeti National Park, Tanzania. *The Journal of Wildlife Management* 79:1014-1021
468

- 469 Dénes FV, Silveira LF, Beissinger SR. 2015. Estimating abundance of unmarked animal
470 populations: accounting for imperfect detection and other sources of zero inflation. *Methods in*
471 *Ecology and Evolution* 6:543-56
472
- 473 Després-Einspenner M-L, Howe EJ, Drapeau P, Kühl HS. Accepted. An empirical evaluation of
474 camera trapping and capture-recapture methods for estimating chimpanzee density. *American*
475 *Journal of Primatology*
476
- 477 Efford MG, Borchers DL, Byrom AE. 2009. Density estimation by spatially explicit capture –
478 recapture: likelihood-based methods. *Modelling Demographic Processes in Marked Populations*
479 (eds D.L. Thompson, E.G. Cooch & M.J. Conroy), pp. 255–269. Springer, New York
480
- 481 Fewster RM, Buckland ST, Burnham KP, Borchers DL, Jupp PE, Laake JL, Thomas L. 2009.
482 Estimating the encounter rate variance in distance sampling. *Biometrics* 65:225-236
483
- 484 Jathanna D, Karanth KU, Johnsingh AJT. 2003. Estimation of large herbivore densities in the
485 tropical forests of southern India using distance sampling. *Journal of Zoology* 261:285-290
486
- 487 Koster SH, Hart JA. 1988. Methods of estimating ungulate populations in tropical forests.
488 *African Journal of Ecology* 26:117-126
489
- 490 Kuehl HS, Todd A, Boesch C, Walsh PD. 2007. Manipulating decay time for efficient large-
491 mammal density estimation: gorillas and dung height. *Ecological Applications* 17:2403-2414

- 492
- 493 Laake JL, Collier BA, Morrison ML, Wilkins RN. 2011. Point-based mark-recapture distance
494 sampling. *Journal of Agricultural, Biological, and Environmental Statistics* 16:389-408
495
- 496 Lynam AJ, Jenks KE, Tantipisanuh N, Chutipong W, Ngoprasert D, Gale GA, Steinmetz R,
497 Sukmasuang R, Bhumpakphan N, Grassman Jr LI, Cutter P. 2013. Terrestrial activity patterns of
498 wild cats from camera-trapping. *Raffles Bulletin of Zoology* 61:407-415
499
- 500 MacKenzie DI, Royle JA. 2005. Designing occupancy studies: general advice and allocating
501 survey effort. *Journal of Applied Ecology* 42:1105-1114
502
- 503 Marini F, Franzetti B, Calabrese A, Cappellini S, Focardi S. 2009. Response to human presence
504 during nocturnal line transect surveys in fallow deer (*Dama dama*) and wild boar (*Sus scrofa*).
505 *European Journal of Wildlife Research* 55:107-115
506
- 507 Marques TA, Buckland ST, Borchers DL, Tosh D, McDonald RA. 2010 Point transect sampling
508 along linear features. *Biometrics* 66:1247-1255
509
- 510 Marques TA, Thomas L, Fancy SG, Buckland ST. 2007. Improving estimates of bird density
511 using multiple-covariate distance sampling. *The Auk* 124:1229-1243
512

- 513 Marshall AR, Lovett JC, White PCL. 2008. Selection of line-transect methods for estimating the
514 density of group-living animals: lessons from the primates. *American Journal of Primatology*
515 70:452–462
- 516
- 517 Miller DL. 2015. Distance: Distance Sampling Detection Function and Abundance Estimation. R
518 package version 0.9.4. <http://CRAN.R-project.org/package=Distance>
- 519
- 520 Newing HS. 1994. Behavioural ecology of duikers (*Cephalophus* spp.) in forest and secondary
521 growth, Taï, Côte d'Ivoire. Ph.D. thesis, University of Stirling, Scotland
- 522
- 523 Newing HS. 2001. Bushmeat hunting and management: implications of duiker ecology and
524 interspecific competition. *Biodiversity and Conservation* 10:99-118
- 525
- 526 N'Goran PK. 2006. Quelques résultats de la première phase du biomonitoring au Parc National
527 de Taï (août 2005 – mars 2006). Ministère de l'Environnement et des Eaux et Forêts, Ministère
528 de l'Enseignement Supérieur et de la Recherche Scientifique, Abidjan, Côte d'Ivoire.
- 529
- 530 Obbard ME, Stapleton S, Middel KR, Thibault I, Brodeur V, Jutras C. 2015. Estimating the
531 abundance of the Southern Hudson Bay polar bear subpopulation with aerial surveys. *Polar*
532 *Biology* 38:1713-25
- 533
- 534 Plumptre AJ. 2000. Monitoring mammal populations with line transect techniques in African
535 forests. *Journal of Applied Ecology* 37:356–368

536

537 R Core Team. 2015. R: A language and environment for statistical computing. R Foundation for
538 Statistical Computing, Vienna, Austria. <http://www.R-project.org/>

539

540 Rovero F, Marshall AR 2004. Estimating the abundance of forest antelopes by line transect
541 techniques: a case from the Udzungwa Mountains of Tanzania. *Tropical Zoology* 17:267-277

542

543 Rovero F, Marshall AR. 2009. Camera trapping photographic rate as an index of density in forest
544 ungulates. *Journal of Applied Ecology* 46:1011-1017

545

546 Rovero F, Zimmermann F, Berzi D, Meek P. 2013. "Which camera trap type and how many do I
547 need?" A review of camera features and study designs for a range of wildlife research
548 applications. *Hystrix, the Italian Journal of Mammalogy* 24:148-156

549

550 Rowcliffe MJ, Carbone C, Jansen PA, Kays R, Kranstauber B. 2011. Quantifying the sensitivity
551 of camera traps: an adapted distance sampling approach. *Methods in Ecology and Evolution*
552 2:464-76

553

554 Rowcliffe, JM, Field J, Turvey ST, Carbone C. 2008. Estimating animal density using camera
555 traps without the need for individual recognition. *Journal of Applied Ecology* 45:1228–1236

556

- 557 Rowcliffe JM, Jansen PA, Kays R, Kranstauber B, Carbone C. 2016. Wildlife speed cameras:
558 measuring animal travel speed and day range using camera traps. *Remote Sensing in Ecology*
559 *and Conservation* 2:84-94
- 560
- 561 Rowcliffe MJ, Kays R, Kranstauber B, Carbone C, Jansen PA. 2014. Quantifying levels of
562 animal activity using camera trap data. *Methods in Ecology and Evolution* 5:1170–1179
- 563
- 564 Saout SL, Chollet S, Chamailié-Jammes S, Blanc L, Padié S, Verchere T, Gaston AJ, Gillingham
565 MP, Gimenez O, Parker KL, Picot D. 2014. Understanding the paradox of deer persisting at high
566 abundance in heavily browsed habitats. *Wildlife Biology* 20:122-35
- 567
- 568 Séquin ES, Jaeger MM, Brussard PF, Barrett RH. 2003. Wariness of coyotes to camera traps
569 relative to social status and territory boundaries. *Canadian Journal of Zoology* 81:2015-2025
- 570
- 571 Sollmann R, Mohamed A, Kelly MJ. 2013*a*. Camera trapping for the study and conservation of
572 tropical carnivores. *The Raffles Bulletin of Zoology* 28:21-42
- 573
- 574 Sollmann R, Mohamed A, Samejima H, Wilting A. 2013*b*. Risky business or simple solution –
575 relative abundance indices from camera trapping. *Biological Conservation* 159:405-412
- 576
- 577 Thomas L, Buckland ST, Rexstad EA, Laake JL, Strindberg S, Hedley SL, Bishop JRB, Marques
578 TA, Burnham KP. 2010. Distance software: design and analysis of distance sampling surveys for
579 estimating population size. *Journal of Applied Ecology* 47:5-14

580

581 Todd AF, Kuehl HS, Cipolletta C, Walsh PD. 2008. Using dung to estimate gorilla density:

582 Modeling dung production rate. *International Journal of Primatology* 29:549-563

583

584 Trailcampro.com. Accessed Aug, 2015. <http://www.trailcampro.com/>

585

586 Wearn OR, Rowcliffe JM, Carbone C, Bernard H, Ewers RM. 2013. Assessing the status of wild

587 felids in a highly-disturbed commercial forest reserve in Borneo and the implications for camera

588 trap survey design. *PLoS ONE* 8:e77598

589

590 Zero VH, Sundaresan SR, O'Brien TG, Kinnaird MF. 2013. Monitoring an Endangered savannah

591 ungulate, Grevy's zebra *Equus grevyi*: choosing a method for estimating population densities.

592 *Oryx* 47:410–419

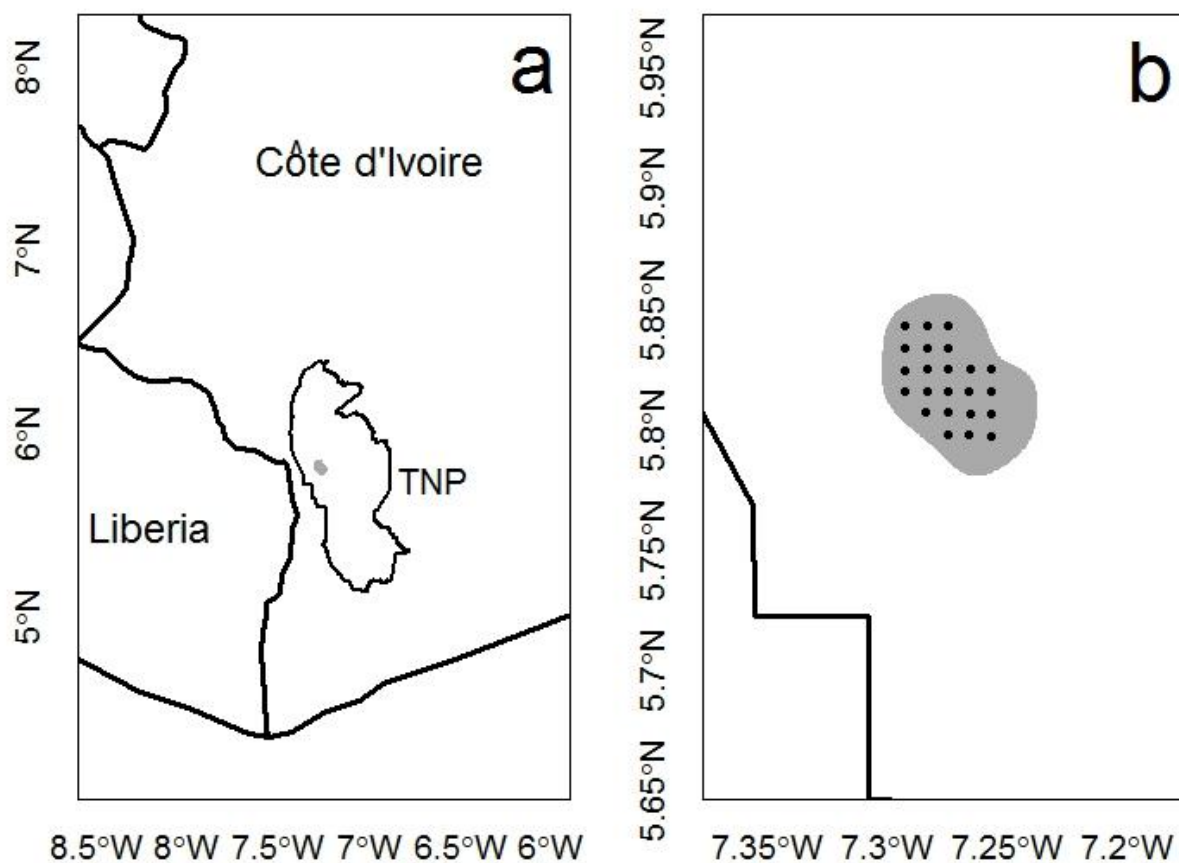
593 Table 1. Densities of Maxwell's duikers in Tai National Park, 2014, estimated using different
 594 methods to account for limited availability for detection. Bootstrap confidence intervals were
 595 calculated using the percentile method.

	Design-based			Bootstrap	
Availability	\hat{D}	CV	95% CI	CV	95% CI
Daytime	10.6	0.27	6.1–18.3	0.40	5.0–21.8
Peak activity	14.5	0.30	7.8–26.9	0.36	6.1–26.9
Active daytime	16.5	0.27	9.5–28.6	0.40	7.7–34.1

596

597

598



599

600 Figure 1. Location of the study area (grey polygon) in Tai National Park (TNP), Côte d'Ivoire,
601 2014 (a), and (b) locations of 23 camera traps deployed in a grid with 1 km spacing within the
602 study area.

603

604

605

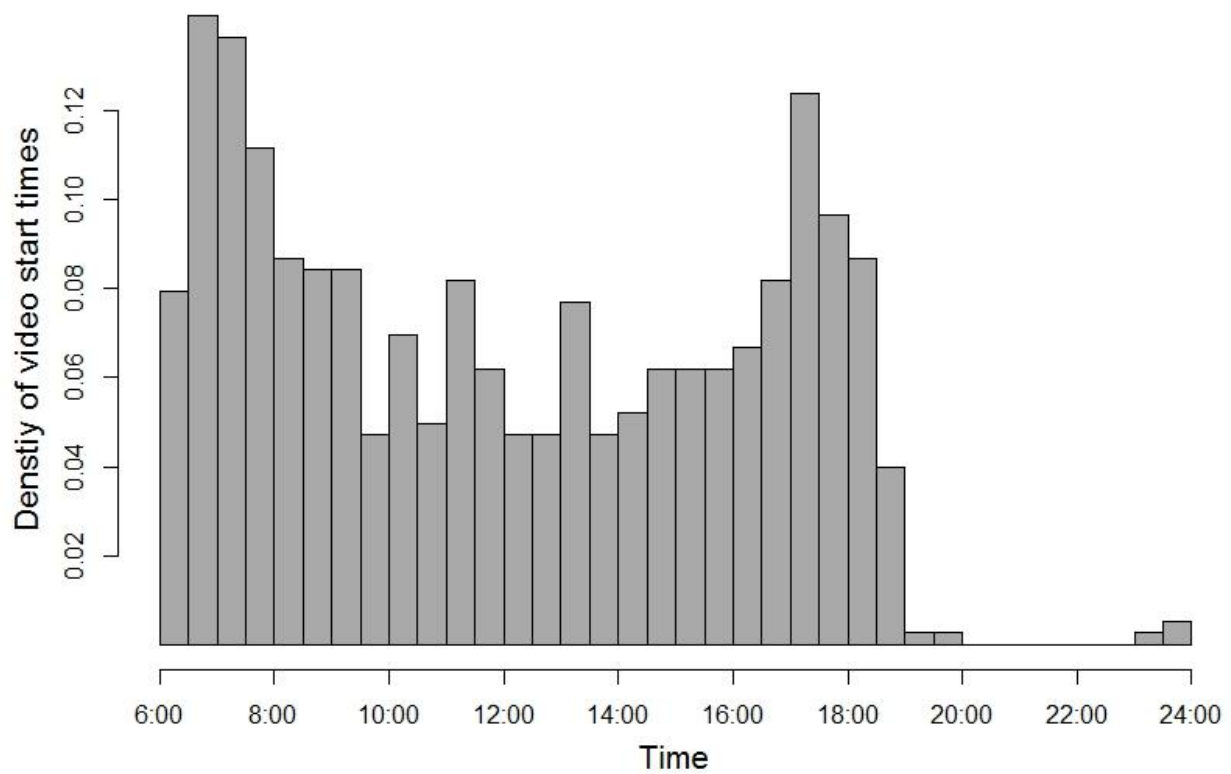
606

607

608

609

610

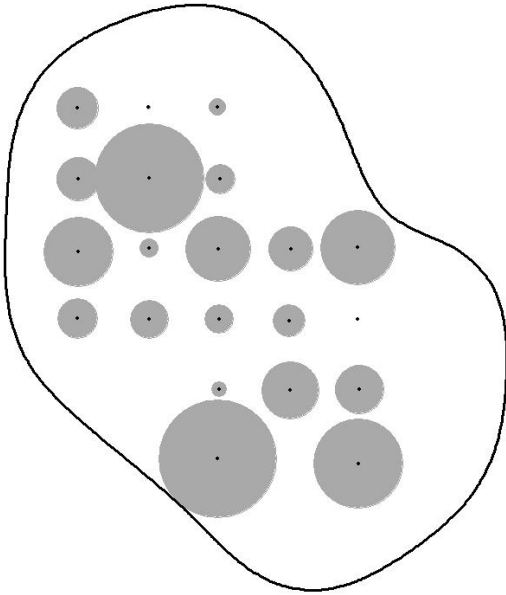


611 Figure 2. Histogram of start times of videos of Maxwell's duikers in Taï National Park, Côte

612 d'Ivoire, 2014.

613

614

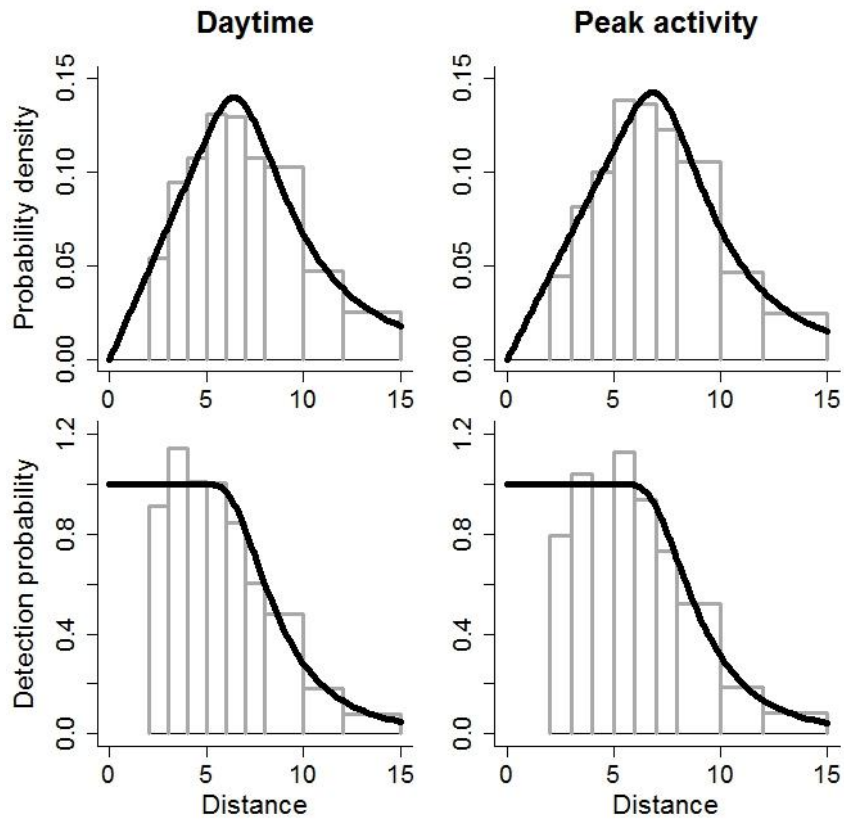


615

616 Figure 3. Variation in encounter rates of Maxwell's duikers among 21 camera trap locations in
617 Taï National Park, Côte d'Ivoire, 2014 (range $0.00 - 1.45 \times 10^{-3}$). The areas of the grey circles
618 are proportional to the encounter rates.

619

620



621 Figure 4. Probability density functions of observed distances (top) and detection probability as a
 622 function of distance (bottom) from hazard-rate point transect models fit to data from Maxwell's
 623 duikers in Tai National Park, 2014, collected during the daytime (left) and during times of peak
 624 activity (right).